

LiNb_{1-x}Ta_xO₃ films prepared by thermal plasma spray CVD

Hironori Yamamoto^{a,*}, Sergei A. Kulinich^b, Kazuo Terashima^{a,b}

^aDepartment of Advanced Materials Science, Graduate School of Frontier Science, The University of Tokyo, Hongo 7-3-1, Bunkyo-ku, Tokyo 113-8656, Japan

^bDepartment of Metallurgy and Materials Science, Faculty of Engineering, The University of Tokyo, Hongo 7-3-1, Bunkyo-ku, Tokyo 113-8656, Japan

Abstract

LiNb_{1-x}Ta_xO₃ films with $x = 0.3$ – 0.7 , epitaxial orientation and good crystallinity were prepared by using thermal plasma spray CVD. Mixtures of metalorganic solutions containing lithium–niobium and lithium–tantalum alkoxides were used as liquid source materials. Preferentially (001)-oriented LiNb_{1-x}Ta_xO₃ films were fabricated on sapphire (001) substrates with deposition rates up to approximately 6 nm/s, which was approximately 100 times as fast as those of most conventional vapor phase deposition methods. LiNb_{1-x}Ta_xO₃ films with $x = 0.5$ achieved a (006) rocking curve full-width at half-maximum value of 0.15 – 0.20° , which is comparable with those of LiNbO₃ and LiTaO₃ films grown by other conventional deposition techniques. This is the first success in preparing LiNb_{1-x}Ta_xO₃ films with $x > 0.33$, good crystallinity and high (001) orientation. © 2001 Elsevier Science B.V. All rights reserved.

Keywords: Lithium niobate–tantalate (LiNb_{1-x}Ta_xO₃); Thermal plasma spray CVD; High-rate deposition; Metalorganic precursor

1. Introduction

Lithium niobate (LiNbO₃, LN) and lithium tantalate (LiTaO₃, LT) are a series of two ferroelectric materials with similar rhombohedral structure and unique pyroelectric, piezoelectric, electro-optic, photoelastic and non-linear optical properties, which make them suitable for acoustic and optical devices [1]. Lithium niobate–tantalate (LiNb_{1-x}Ta_xO₃, LNT) is their solid solution and possesses intermediate properties, which vary with the $x = \text{Ta}/(\text{Nb} + \text{Ta})$ ratio, from those of LN at $x = 0$ to those of LT at $x = 1$. This makes it a more attractive material than the pure compounds, since its properties can be tuned to meet engineering

specifications, which is very important for practical application [2].

With the progress of thin film technology and the growth of high-quality thin films, LN, LT and LNT can have high potential for numerous applications, such as surface wave acoustic and optical waveguide devices, second-harmonic generators, and holographic memory using the photorefractive effect [2]. During the past decade, a large number of deposition techniques for LN and LT films have been explored, including metalorganic chemical vapor deposition (MOCVD) [3–5], liquid phase epitaxy (LPE) [6,7], ion plating [8], sol–gel processing [9–11], pulsed laser deposition (PLD) [12–14], etc. In contrast, there have been only a few reports on LNT film deposition [15,16]. Kawaguchi et al. [15] reported LNT film growth on LN(001) substrates with $x = 0$ – 0.4 using the LPE method. In their experiment, film crystallinity (FWHM) degraded markedly when $x > 0.3$, corresponding to the increase of lattice mismatch and growth temperature. Moreover,

* Corresponding author. Tel.: +81-3-5841-7101; fax: +81-3-5841-7103.

E-mail address: yamamoto@terra.mm.t.u-tokyo.ac.jp (H. Yamamoto).

Cheng et al. [16] prepared highly *c*-oriented LNT films with $x < 0.33$ on Si(111) substrates using the sol-gel technique. They also found that the degree of orientation was relatively low when $0.5 < x < 1$.

Recently, Yamaguchi et al. [17] demonstrated the effectiveness of the thermal plasma spray (TPS) CVD method for high-rate and large-area deposition of LN films on (110) sapphire substrates. Due to its high reactivity and particle density, high growth rate and easy compositional control by using liquid initial material, TPS CVD can be an advantageous technique for the deposition of various multi-component films [17,18]. In our previous study, we also applied this method to the high-rate (up to 1.2 nm/s) deposition of LNT films with $x = 0.4$ –0.5 on sapphire (001) [19]. The aim of this work was to study the synthesis of *c*-axis oriented LNT films within wider range of x (0.3–0.7) and at various growth rates up to approximately 8 nm/s.

2. Experimental procedures

2.1. Starting materials

As mentioned in our previous work [19], various mixtures of liquid lithium–niobium and lithium–tantalum alkoxide metalorganic solutions commercially available for dip coating [LiNb(OR)₆ and LiTa(OR)₆ in 3-methylbutyl acetate as a solvent, Kojundo Chemical Lab. Co., Japan] were used as liquid precursors. The concentration of metals (Li and Nb or Li and Ta) in individual precursor solutions, which were then mixed in appropriate ratios, corresponded to 3 wt.% LiNbO₃ and 3 wt.% LiTaO₃, respectively. In this study, mixtures with molar Nb/Ta ratios of 3:7, 4:6, 5:5, 6:4 and 7:3 were used as initial materials.

As-received optically polished sapphire (001) single-crystal plates (10 × 10 × 0.5 mm in size, Earth Chemicals Ltd., Japan) were used as substrates. Prior to film growth, they were ultrasonically cleaned and rinsed with acetone and ethanol.

2.2. Experimental setup

Fig. 1 shows a schematic diagram of the experimental setup for TPS CVD, which is almost the same as the thermal plasma flash evaporation apparatus described previously [20,21], except for the liquid raw material feeding system, additional substrate vacuum pump for holding the substrate and an induction coil to initiate plasma generation. The system consists essentially of three parts: (1) a radio-frequency (RF) thermal plasma reactor; (2) a liquid metalorganic precursor feeding system; and (3) a water-cooled stainless-steel substrate holder with an optical fiber for a direct temperature measurement in real time. In contrast to previous work

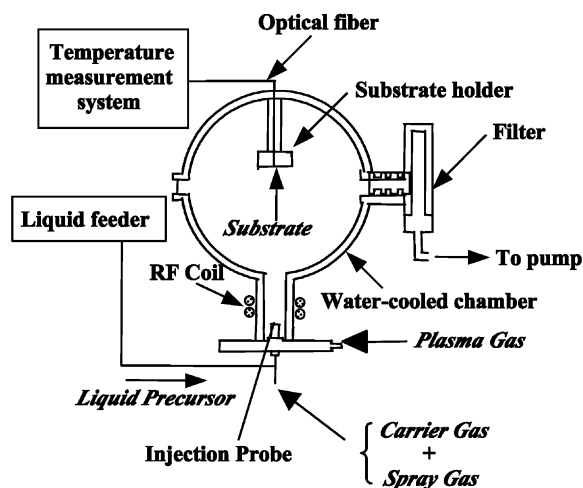


Fig. 1. Experimental setup.

by Yamaguchi et al. [17], in the present setup, a plasma torch was set at the bottom of the chamber, and consequently the plasma was blown upward to prevent large droplets of the liquid raw material from falling down. The substrate temperature was measured by detecting infrared radiation from the reverse side of the substrate through an optical fiber, which made it possible to monitor the substrate temperature directly in real time.

The liquid precursors containing metalorganic compounds were introduced as a mist into the oxygen–argon plasma through the stainless-steel probe tube. Once in the plasma, the liquid precursors were evaporated, decomposed, and reacted in the boundary layer over the substrate to form LNT deposit. A summary of the experimental conditions is presented in Table 1.

2.3. Analyses

The crystallinity, phase and orientation of the films were determined by X-ray diffraction (XRD) using θ – 2θ and θ scans. The relationship between crystal axes of films and in-plane vectors of sapphire was analyzed based on an X-ray pole measurement. Film thickness and surface morphology were examined by

Table 1
Summary of experimental conditions

Power	42–53 kW
Pressure	150 torr
O ₂ tangential gas flow rate	45.0 l/min
Ar carrier gas flow rate	3.0 l/min
Ar spray gas flow rate	3.6 l/min
Ar inner gas flow rate	5.0 l/min
Liquid feeding rate (<i>R</i>)	0.5–10.0 ml/min
Starting substrate temperature	630–660°C
Torch–substrate distance (<i>L</i>)	370 mm
Deposition time	20–300 s

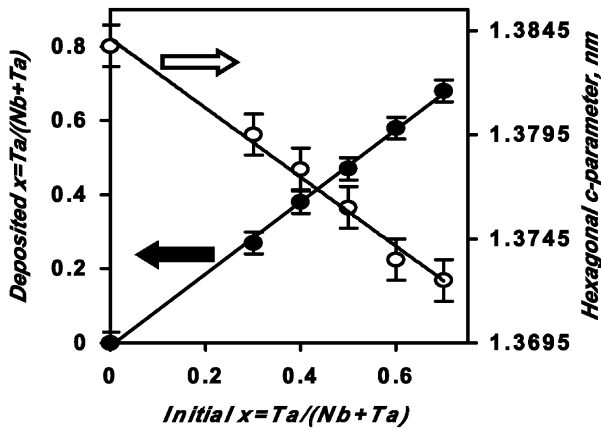


Fig. 2. Variation of the $x = \text{Ta}/(\text{Nb} + \text{Ta})$ ratio in film as a function of the initial $x = \text{Ta}/(\text{Nb} + \text{Ta})$ ratio in liquid source. Variation of the hexagonal unit cell c -parameter is also indicated.

scanning electron microscopy (SEM). The composition of the films was analyzed by inductively-coupled plasma atomic emission spectroscopy (ICP-AES) after the samples had been completely dissolved in HF and H_2SO_4 .

3. Results and discussion

3.1. Compositional variation

Fig. 2 shows the variation of film composition with source composition. These data were obtained by the ICP-AES method. As shown in Fig. 2, the Ta content ratio in the films, $x = \text{Ta}/(\text{Nb} + \text{Ta})$, increased linearly with increasing initial Ta content in the source material and was very close to the latter. This means that the film composition can be precisely controlled by varying the initial liquid precursor composition.

The c parameters for the LNT films with various Ta content ratios calculated from the XRD patterns are also indicated in Fig. 2; the data for several LN films (LNT with $x = 0$) deposited under similar conditions are presented. These results are in good agreement with those of ICP-AES measurement, since a more Ta-rich material should show a smaller c parameter. According to The Joint Committee on Powder Diffraction Standard (JCPDS, PDF Nos. 20-631, 38-1252 and 29-836) data for bulk materials, this parameter decreases from 1.3862 nm for LN to 1.3815 nm for LNT with $x = 0.5$ to 1.3755 nm for LT. Somewhat smaller c lattice parameters of LNT films compared with those of bulk materials are believed to be due to the planar tensile stress of the (001) plane. This stress results from a large lattice mismatch and a large difference between the thermal expansion coefficients of LNT and sapphire. As demonstrated by Veignant et al. [12], the above mismatch parameter between LN film and the sapphire (001) substrate is 7.7% at room temperature and goes up to 8.6% at the $T_{\text{sub}} = 750^\circ\text{C}$; this must also be true for LNT films.

3.2. Orientation and crystallinity

Because of its anisotropic electro-optic properties, the control of LNT film orientation is very important. The c -axis-oriented LNT films possess a single coefficient element, such as non-linear and piezoelectric (d_{33}), electro-optic (γ_{33}), permittivity (ϵ_{33}), and refractive index (n_{33}), which are essential for integrated optics applications [1,16].

According to Hu et al. [14], a convenient parameter for describing the degree of c -axis orientation of the LNT films can be defined as

$$f = \frac{I_r(006) - I_r^{\text{powder}}(006)}{1 - I_r^{\text{powder}}(006)},$$

where relative intensity $I_r(006)$ is the intensity of the (006) peak normalized by the intensity sum of all the peaks of LNT between $2\theta = 20\text{--}60^\circ$. For randomly oriented polycrystalline films, as in the case of powders, the degree of c -axis orientation (f) is equal to 0; for completely c -axis oriented LNT films, $f = 1$; and for partially c -axis oriented films, f falls between zero and one [14,16]. Fig. 3 shows diffraction patterns from two LNT films ($x = 0.5$) with almost perfect and high c -axis orientations, $f = 0.995$ and $f = 0.932$, respectively. These films were deposited under similar conditions, except for liquid feeding rate R , and have a similar thickness of approximately 160 nm, but their degrees of c -axis orientation are slightly different due to the growth rate effect described below. Also, the XRD patterns in Fig. 3 indicate that all LNT films grown in this study under various conditions of T_{sub} and R were generally single-phase samples.

Since the substrate temperature (T_{sub}) and the liquid feeding rate (R) are crucial parameters in thin film fabrication, an experimental investigation on the effects of T_{sub} and R on the film orientation and crystallinity is of prime importance. In our experiment, initial T_{sub} was approximately $30\text{--}70^\circ\text{C}$ lower than deposition T_{sub} . This was due to additional substrate heating by the chemical energy of oxidation after the liquid metalorganic precursor had been injected into the plasma.

Fig. 4a shows the degree of c -axis orientation as a function of the starting (injection) T_{sub} for the series of 150–170-nm thick LNT films with $x = 0.5$ deposited using $R = 1.0$ ml/min. As this temperature rises to over 650°C , the orientation degree (f) gradually decreases. Fig. 4b shows the f and the (006) rocking curve FWHM value as functions of liquid feeding rate R for the LNT 150–170-nm thick films ($x = 0.5$) deposited using the same starting T_{sub} of 650°C . As R increases, f approaches 1 and the rocking curve FWHM value

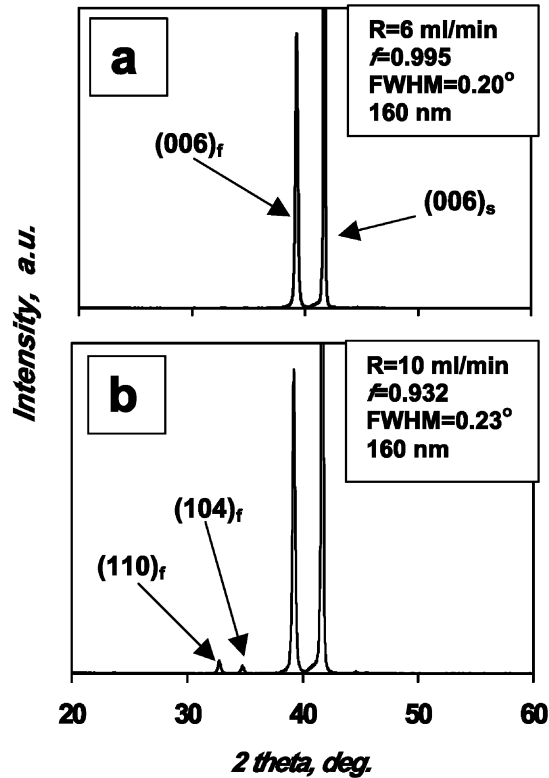


Fig. 3. XRD patterns of LNT films ($x = 0.5$, 160 nm thick) with (a) $f = 0.995$ and (b) $f = 0.932$ prepared at $R = 6.0$ and 10.0 ml/min, respectively. Subscripts 'f' and 's' denote film and substrate peaks, respectively.

decreases, reaching a value of the order of $0.15\text{--}0.20^\circ$ at $R = 4.0\text{--}8.0$ ml/min. Both temperature and feeding rate effects on the LN film orientation and crystallinity were reported by Lee and Feigelson and can be explained in terms of surface free-energy anisotropy [4]. When T_{sub} increases, adspecies can attain sufficient surface mobility to arrange themselves into grains with the lowest surface energy (012) planes parallel to the substrate surface. This can be suppressed by using an increased growth rate, since in such a case the adspecies cannot diffuse farther along the growth interface and cannot form energetically more favorable sites with reduced surface energy. Thus, at a faster growth rate (higher R) the c -axis texturing is improved, which results in better crystalline alignment of the films [4]. Some decrease in the LNT film crystallinity and orientation at $R > 8.0$ ml/min can be attributed to the occurrence of gas phase nucleation at higher feeding rates and subsequent polycrystalline film formation. This is in agreement with Fig. 3, where the sample deposited at $R = 10.0$ ml/min exhibits some fraction of grains with (110) and (104) orientations, whereas the sample deposited at $R = 6.0$ ml/min has almost perfect (001) orientation.

The epitaxial properties of the LNT film ($x = 0.5$) grown at $R = 1.0$ ml/min for 5 min with starting $T_{\text{sub}} =$

640°C and deposition $T_{\text{sub}} = 705^\circ\text{C}$ are shown in Fig. 5. There are two groups of LNT (012) poles, each of them having three-fold symmetry. The relative intensity ratio between these two groups was determined from the (208) plane ϕ -scan and was less than 1:10. This suggests that the c -axis-oriented LNT film was grown with epitaxial orientation, however, there are less than 9% of twinned grains which are rotated by 60° around the film normal. As demonstrated in our previous work [19], the number of 60° -rotated grains could be reduced by using a higher deposition T_{sub} .

While in previous studies [15,16] serious degradation of LNT film crystallinity and orientation occurred when $x > 0.33$, in the present experiment, we did not observe any obvious worsening of the film quality, and highly c -axis-oriented 150–400-nm thick LNT films with FWHM values of approximately $0.15\text{--}0.35^\circ$ could be

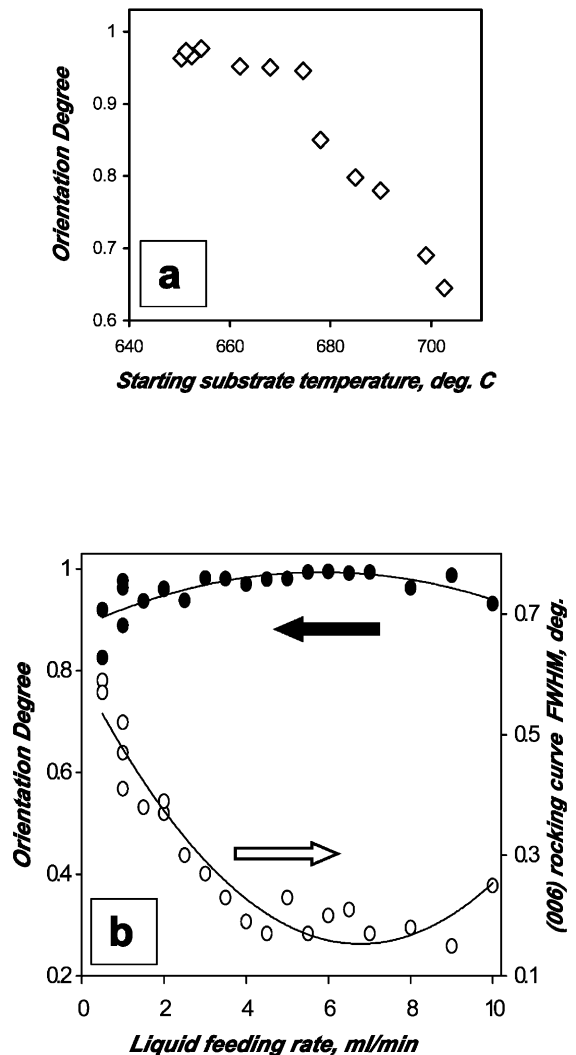


Fig. 4. The change of LNT ($x = 0.5$) 150–170-nm thick film degree of orientation as a function of (a) the starting T_{sub} and (b) liquid feeding rate R at the starting $T_{\text{sub}} = 650^\circ\text{C}$ (the change of rocking curve FWHM value for the same films is also shown).

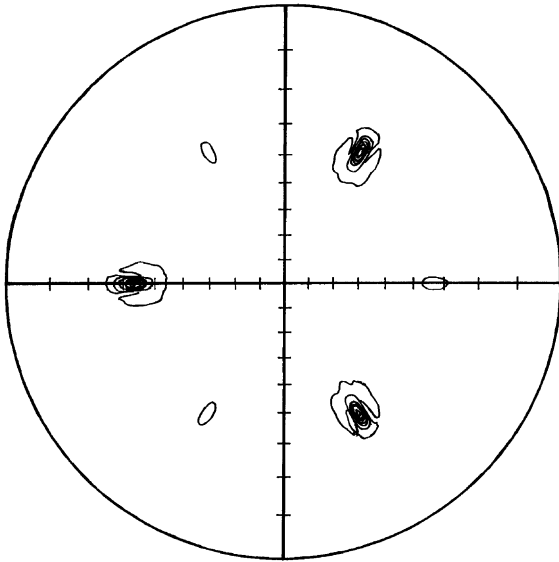


Fig. 5. Pole figure of 240-nm thick LNT film with $x = 0.5$, where normals of the (012) planes of LNT and sapphire substrate are indicated. From the (208) plane ϕ -scan, the ratio of weak intensity LNT group to strong intensity LNT group is less than 1:10.

deposited throughout the entire Ta composition range investigated.

3.3. Film thickness and morphology

For LNT films (Fig. 4b) deposited with various liquid feeding rate R , the growth rate estimated from cross-sectional SEM images reached the value of 6–8 nm/s at $R = 8$ –10 ml/min. When optimal $R = 4$ –8 ml/min was applied, it was estimated to be approximately 4–6 nm/s. The latter value (4–6 nm/s) was approximately 100 times as fast as those of most conventional vapor phase deposition methods (0.003–0.08 nm/s for MOCVD [3–5], 0.04 nm/s for ion plating [8] and 0.17 nm/s for PLD [12]).

$\text{LiNb}_{1-x}\text{Ta}_x\text{O}_3$ films with thicknesses of at least 400 nm and rocking curve FWHM values of 0.15–0.35° could be obtained throughout the entire compositional range studied, $0.3 < x < 0.7$. As mentioned above, film growth was accompanied by an increase of T_{sub} depending on deposition time, material input rate R and initial T_{sub} . Therefore, at a somewhat elevated temperature, film crystallinity and orientation, which are functions of surface mobility, deteriorated slightly in the case of thicker films. Taking this into account, the heating/cooling system must be improved in order to obtain stable T_{sub} and allow further progress in thick film preparation.

As was demonstrated in our previous work [19], the roughness of high-rate-deposited LNT films is somewhat higher than those of the LN and LT films with the best surface. Therefore, further experimental studies on nucleation and growth mechanisms are necessary in

order to decrease the grain size and improve the surface morphology such as the roughness of the LNT films produced.

4. Conclusions

The thermal plasma spray CVD method was applied to the preparation of epitaxially oriented $\text{LiNb}_{1-x}\text{Ta}_x\text{O}_3$ thin films with $x = 0.3$ –0.7. Uniform mixtures of metalorganic solutions containing lithium–niobium and lithium–tantalum alkoxides were used as liquid source materials. The XRD results indicate that the substrate temperature and liquid feeding rate are the key process parameters for various orientations and crystal qualities of films. Preferentially (001)-oriented $\text{LiNb}_{1-x}\text{Ta}_x\text{O}_3$ films with good crystallinity were fabricated on (001) sapphire substrates with deposition rates up to 6 nm/s. $\text{LiNb}_{1-x}\text{Ta}_x\text{O}_3$ films with $x = 0.5$ exhibited a (006) rocking curve full-width at half-maximum value of 0.15–0.20°, which is comparable with those of LiNbO_3 and LiTaO_3 films grown by other conventional deposition techniques. This is the first success in preparing $\text{LiNb}_{1-x}\text{Ta}_x\text{O}_3$ films with $x > 0.33$, good crystallinity and high (001) orientation. In contrast to previous reports on LNT films prepared using LPE and sol-gel techniques, the film crystallinity and degree of orientation did not degrade markedly when $x > 0.33$. Further experimental studies on the mechanisms of grain nucleation and growth are necessary in order to decrease surface roughness.

Acknowledgements

The authors are extremely grateful to Professor Toyonobu Yoshida for his discussions and encouragement. We also thank Mr Hisashi Komaki (JEOL Ltd.) for the development of the liquid feeding system and the plasma chamber. This work was supported by the Japan Society for the Promotion of Science under the program ‘Research for the Future’ (97R15301).

References

- [1] A. Rauber, in: E. Kaldis (Ed.), *Current Topics in Material Science* 1, North Holland, Amsterdam, 1978, p. 481.
- [2] R.E. Cohen, *J. Phys. Chem. Solids* 61 (2000) 139.
- [3] A.A. Wernberg, H.J. Gysling, G. Braunstein, *J. Cryst. Growth* 140 (1994) 57.
- [4] S.Y. Lee, R.S. Feigelson, *J. Mater. Res.* 14 (1999) 2662.
- [5] S.Y. Lee, R.S. Feigelson, *J. Cryst. Growth* 186 (1998) 594.
- [6] A. Yamada, H. Tamada, M. Saitoh, *J. Cryst. Growth* 132 (1993) 48.
- [7] T. Kawaguchi, K. Mizuuchi, T. Yoshino, M. Imaeda, K. Yamamoto, T. Fukuda, *J. Cryst. Growth* 203 (1999) 173.
- [8] H. Matsunaga, H. Ohno, Y. Okamoto, Y. Nakajima, *J. Cryst. Growth* 99 (1990) 630.
- [9] S. Ono, O. Bose, W. Unger, Y. Takeichi, S. Hirano, *J. Am. Ceram. Soc.* 81 (1998) 1749.

- [10] K. Terabe, A. Gruverman, Y. Matsui, N. Iyi, K. Kitamura, J. Mater. Res. 11 (1996) 3152.
- [11] K. Nashimoto, M.J. Cima, Mater. Lett. 10 (1991) 348.
- [12] F. Veignant, M. Gandais, P. Aubert, G. Garry, J. Cryst. Growth 196 (1999) 141.
- [13] Z.C. Wu, W.S. Hu, J.M. Liu, M. Wang, Z.G. Liu, Mater. Lett. 34 (1998) 332.
- [14] W.S. Hu, Z.G. Liu, Z.C. Wu, J.M. Liu, X.Y. Chen, D. Feng, Appl. Surf. Sci. 141 (1999) 197.
- [15] T. Kawaguchi, H. Kitayama, M. Imaeda, S. Ito, K. Kaigawa, T. Taniuchi, T. Fukuda, J. Cryst. Growth 169 (1996) 94.
- [16] S.D. Cheng, C.H. Kam, Y. Zhou, X.Q. Han, W.X. Que, Y.L. Lam, Y.C. Chan, J.T. Oh, W.S. Gan, Thin Solid Films 365 (2000) 77.
- [17] N. Yamaguchi, T. Hattori, K. Terashima, T. Yoshida, Thin Solid Films 316 (1998) 185.
- [18] S. Shimada, M. Yoshimatsu, H. Nagai, M. Suzuki, H. Komaki, Thin Solid Films 370 (2000) 137.
- [19] T. Majima, H. Yamamoto, S.A. Kulinich, K. Terashima, J. Cryst. Growth 220 (2000) 336.
- [20] Y. Takamura, K. Hayasaki, K. Terashima, T. Yoshida, Plasma Chem. Plasma Proc. 16 (1996) 141S.
- [21] K. Hayasaki, Y. Takamura, N. Yamaguchi, K. Terashima, T. Yoshida, J. Appl. Phys. 81 (1997) 1222.